Structural Basis of Cyclic 1,3-Diene Forming Acyl-Coenzyme A Dehydrogenases

Johannes W. Kung,[a] Anne-Katrin Meier,[a] Max Willistein,[a] Sina Weidenweber,[b] Ulrike Demmer,[b] Ulrich Ermler,*[b] and Matthias Boll*[a]

The biologically important, FAD-containing acyl-coenzyme A (CoA) dehydrogenases (ACAD) usually catalyze the *anti*-1,2-elimination of a proton and a hydride of aliphatic CoA thioesters. Here, we report on the structure and function of an ACAD from anaerobic bacteria catalyzing the unprecedented 1,4-elimination at C3 and C6 of cyclohex-1-ene-1-carboxyl-CoA (Ch1CoA) to cyclohex-1,5-diene-1-carboxyl-CoA (Ch1,5CoA) and at C3 and C4 of the latter to benzoyl-CoA. Based on high-resolution Ch1CoA dehydrogenase crystal structures, the unorthodox reactivity is explained by the presence of a catalytic aspartate base (D91) at C3, and by eliminating the catalytic glutamate base at C1. Moreover, C6 of Ch1CoA and C4 of Ch1,5CoA are positioned towards FAD-N5 to favor the biologically relevant C3,C6- over the C3,C4-dehydrogenation activity. The C1,C2-dehydrogenation activity was regained by structure-inspired amino acid exchanges. The results provide the structural rationale for the extended catalytic repertoire of ACADs and offer previously unknown biocatalytic options for the synthesis of cyclic 1,3-diene building blocks.

Members of the acyl-coenzyme A (CoA) dehydrogenase (ACAD) family play a crucial role in the catabolism of fatty and amino acids in all domains of life.[1] Moreover, they are involved in numerous bacterial metabolic pathways such as the degradation of aromatic compounds[2,3] or steroids,[4–6] fermentations,[7,8] synthesis of natural products,[9–11] and carbon fixation,[12] among others. ACADS usually catalyze the 1,2-dehydrogenation of acyl-CoA to the corresponding *trans*-2-enoyl-CoA; electrons are transferred to oxidized electron-transferring flavoproteins (ETF).[13] The two C–H bonds are cleaved by (i) abstraction of a proton from the C1-position by a highly conserved glutamyl residue with a high pK_a of around 8, and (ii) hydride transfer from the C2 to the N5 of the FAD isoalloxazine ring. Whether the C–H-bonds are ruptured sequentially via a true enolate transition state, stabilized by the thioester functionality, or concertedly is a matter of debate.[13–15]

According to amino acid sequence similarities and substrate specificities ACADs are categorized into several classes acting on linear or branched CoA-ester substrates with differing chain lengths.[1] The vital glutamate residue is present in all ACADs which, however, protrudes from different regions of the polypeptide chain towards C1.[13,14] The ACAD member 3-sulfinopropionyl-CoA desulfinase does not catalyze a dehydrogenation reaction and lacks the catalytic glutamyl residue.[16]

Recently, we identified and initially characterized cyclohex-1-ene-1-carboxyl-CoA dehydrogenases (Ch1DH) from the strictly anaerobic Deltaproteobacteria *Syntrophus aciditrophicus*[17] and *Geobacter metallireducens*.[18,19] The FAD-containing enzymes play a key role in fermentative cyclohexane carboxylic acid formation[17] or degradation,[18] and belong to the short-chain class of ACADs. Ch1DHs catalyze the C3,C6-dehydrogenation (a formal 1,4-dehydrogenation) of cyclic Ch1CoA (**1**) to cyclohexa-1,5-diene-1-carboxyl-CoA (Ch1,5CoA, **2**). In contrast, they do not catalyze a canonical 1,2-dehydrogenation (Scheme 1). Next to this biologically relevant reaction, Ch1DH catalyzed the C3,C4-dehydrogenation from **2** yielding benzoyl-CoA **3**, albeit at a lower rate and with a higher K_m-value for the substrate.[17] According to the reactivity of the CoA ester substrates, a proton is likely abstracted from C3, and a hydride is transferred from C6 or C4. Such catalytic capabilities are unique among ACADs. Here, we analyzed the non-canonical ACAD reaction types by

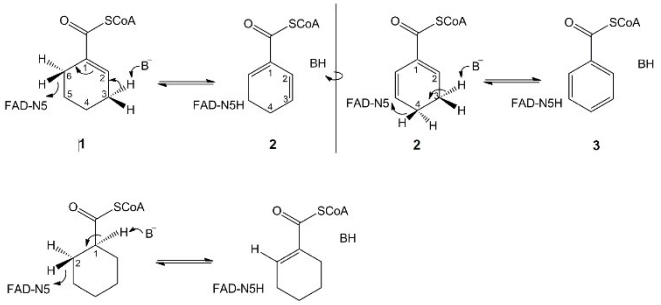

Scheme 1. Reactions catalyzed and not catalyzed by Ch1DH from *G. metallireducens*. Upper panel: C3,C6-dehydrogenation from **1** to **2**, and the C3,C4-dehydrogenation from **2** to **3** catalyzed by Ch1DH. Lower panel C1,C2-dehydrogenation not catalyzed by Ch1DH.

[a] *Dr. J. W. Kung, A.-K. Meier, Dr. M. Willistein, Prof. Dr. M. Boll*
Faculty of Biology – Microbiology
Albert-Ludwigs-Universität Freiburg
Schänzlestrasse 1, 79104 Freiburg (Germany)
E-mail: matthias.boll@biologie.uni-freiburg.de
[b] *Dr. S. Weidenweber, U. Demmer, Dr. U. Ermler*
Max-Planck-Institute for Biophysics
Max-von-Laue-Strasse 3, 60438 Frankfurt (Germany)
E-mail: Uli.Ermler@mpibp-frankfurt.mpg.de

Supporting information for this article is available on the WWW under https://doi.org/10.1002/cbic.202100421

combining structural and structure-inspired mutational methodologies.

The gene encoding Ch1DH from *G. metallireducens* (Gmet_3306) was heterologously expressed with an N-terminal His-tag, and the enzyme produced was purified by Ni-affinity chromatography as described (Figure S1).[18] The homotetrameric enzyme contained 0.72 FAD per 41-kDa subunit and exhibited both, Ch1CoA dehydrogenating (4.2 ± 0.2 μmol min^{-1} mg^{-1}) and Ch1,5CoA dehydrogenating activities (0.89 ± 0.1 μmol min^{-1} mg^{-1}) in the presence of the electron acceptor ferrocenium hexafluorophosphate (Figure S1).

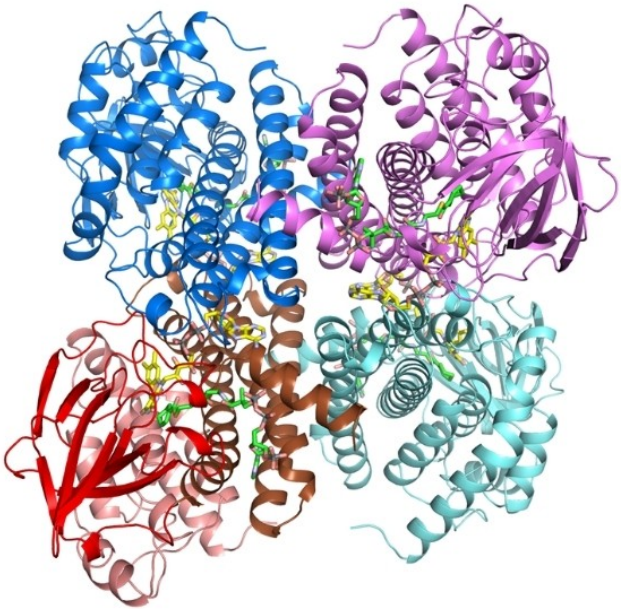

Figure 1. Overall Ch1DH-Ch1,5CoA complex structure at 1.5 Å. Three subunits of the homotetramer are drawn blue, violet and aquamarine and the fourth subunit according to its domain composition (N-terminal helix domain, salmon; C-terminal helix domain, brown; intermediate domain, red). FAD (C in yellow) and Ch1CoA/Ch1,5CoA (C in green) are shown as sticks.

Ch1DH was structurally characterized in the as isolated state at 2.0 Å resolution (PDB-code 7P98) as well as in complex with Ch1CoA or Ch1,5CoA at resolutions of 1.65 Å (PDB-code 7P9X) and 1.5 Å (PDB-code 7P9A), respectively (Figure 1, Table S1). A comparison with standard ACADs indicates a highly similar overall architecture regarding the tetrameric state and the fold of the subunits each composed of a helical N-terminal (1–117), C-terminal (228–380) and intermediate sheet domain (118–227) (Figure 1). The rms deviation between Ch1DH and the most closely related family members rat short chain ACAD (1jqi) and human MCAD (1t9g) are with 1.0–1.1 Å very small (380 of 384/386 C_α atoms).[20,21] The conserved binding site of FAD is located between the intermediate and C-terminal domains of two subunits in an elongated cavity with the isoalloxazine ring adopting a butterfly conformation (Figure 2).

Binding of Ch1CoA or Ch15CoA at the active site induce no larger conformational changes. The CoA moiety is fixed by multiple, mostly invariant interactions with the polypeptide including those between the carbonyl oxygen of the CoA thioester and Thr363-NH and an FAD-ribitol hydroxyl that are crucial for decreasing the pK_a value of C3 (Figure 2). A constriction formed by G130, L133, L238, R242, G364 and the FAD ribitol completely locks the active site upon substrate binding in a reaction chamber encapsulated from bulk solvent. In the substrate-free structure, Leu238 and Arg242 are displaced to enable the substrate to enter the chamber. The Ch1CoA/Ch1,5CoA rings adopt a half-chair like conformation that despite the high occupancy and the excellent electron density cannot be distinguished (after 180 °C rotation, Scheme 1). The presence of chair-shaped ChCoA or planar benzoyl-CoA can be excluded (Figure 3).

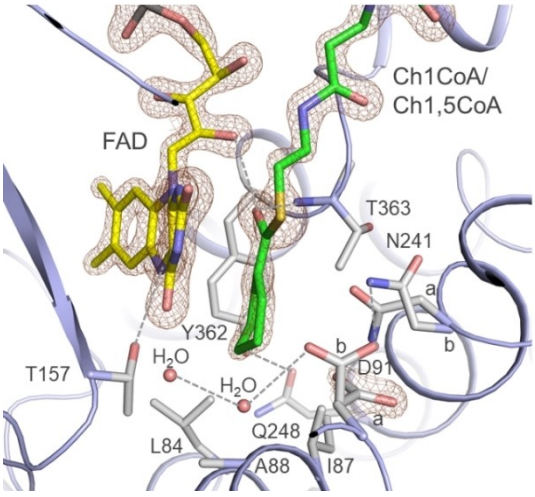

Figure 2. The Ch1CoA/Ch1,5CoA binding site. The ring moiety is embedded in a locked reaction chamber at the cleft bottom and lined up by the isoalloxazine ring, L84, I87, A88, D91, T157, N241, Q248, Y362 and T363 (shown as sticks). The two conformations of D91 and N241 are marked by a and b. The $2F_o-F_c$ electron density (brown) of FAD and Ch1CoA/Ch1,5CoA are contoured at 2.5σ; that of D91 side chain at 1σ.

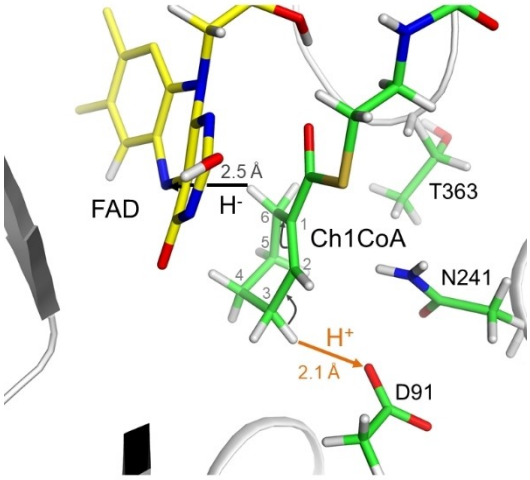

Figure 3. Pre-turnover active site architecture of the C3,C6-elimination reaction. The hydrogens are modelled based on the reliable ring geometry. The hydride transfer is marked with a black arrow; the proton transfer with an orange arrow.

D91 is the only catalytic base candidate in the active site of Ch1DH. It protrudes from an exposed loop of the broken helix 79:98 of the N-terminal domain towards the six-membered ring and adopts two side chain conformations. In the first conformation, its OD2 atom has an ideal distance and angle to the proS C3 hydrogen (O···H: 2.1 Å, (O···H–C: 154°). It is worth to note that the OD2 lone pair is in the *anti* form relative to the carbonyl OD1 although the *syn* form is estimated to be 104-fold more favorable for protonation.[22] However, in Ch1DH the more basic *syn* lone pair is saturated by a hydrogen-bond with the Asn241 ND2, which fixes the conformation of the carboxylate group. In the second conformation, the OD2 group sits geometrically unfavorable for proton abstraction (2.8 Å, 117°). Its carboxylate group is hydrogen-bonded with water molecules buried inside the protein matrix. Both side chain conformations are convertible into each other by a rotation around the C_α–C_β bond. In the substrate-free Ch1DH structure, D91 is in the active conformation.

The *re*-sides of the isoalloxazine and Ch1CoA/Ch1,5CoA rings face each other. The distance between N5 and C6 of 3.2 Å and an N···proR H–C angle of 127° is ideal for the C3,C6-dehydrogenation but only suboptimal for the C3,C4-dehydrogenation (N5-C4 distance: 3.9 Å and N···H–C angle: 135°). For the latter reaction, we assume an additional shift of the six-membered ring relative to the isoalloxazine ring in the range of 0.5 Å, either by thermal vibrations and/or an alternative transient binding towards the entrance of the cavity. Despite the assumed high activation energy, the C3,C4-elimination activity can be rationalized by the strong thermodynamic driving force to form the aromatized benzoyl-CoA.

The high accuracy of the ring atom coordinates and electron density also permit to definitive classification of the reaction as a stereospecific *trans*-dehydrogenation. At least for the C3,C6-elimination, a concerted hydride and proton transfer scenario would be in line with the found isoalloxazine, substrate and D91 geometry (Figure 3). In addition, the structural data implicate that ChCoA cannot be 1,2-dehydrogenated as the D91-OD2 to C1 distance of 4.5 Å is too long for proton transfer. Altogether, the structural data convincingly explain the region- and stereospecificity of the C3,C6- and C3,C4-dehydrogenation reactions. They visualize the structure of the precatalytic enzyme : substrate complex that to our best knowledge is exceptional among ACAD family members in terms of distance and angle accuracy of the proton- and hydride-transferring groups (Figure 3).

Amino acid sequence comparisons revealed that the proposed catalytic base D91 is invariant in Ch1DHs, whereas all others ACADs contain a catalytic glutamate (Figure S2). In short- and medium chain ACADs, the latter is located prior to the final helix of the C-terminal domain,[13] whereas in ACADs converting long chain fatty acids and branched substrates this residue is found after the first helix of the C-terminal domain of the enzyme (Figure 4).[14] In Ch1DHs, the space of the catalytic glutamate is occupied by asparagine and threonine (N241 and T263 in *G. metallireducens* Ch1DH, Figure S2). In turn, its catalytic D91 is replaced in all other ACADs by hydrophobic residues. A superposition of ACAD-acyl-CoA complexes indicates that the helices 79:98, 229:266 and 349:378 (Ch1DH nomenclature) are slightly displaced relative to each other and partially disrupted (Figure 4). In CH1DH, residues preceding D91 are lacking (Figure S2), and the invariant G92 maybe essential to optimally position D91 towards C3 of Ch1CoA. In summary, the ACAD family serves as an excellent example how the gain and loss of reactivities is accomplished by a few amino acid exchanges.

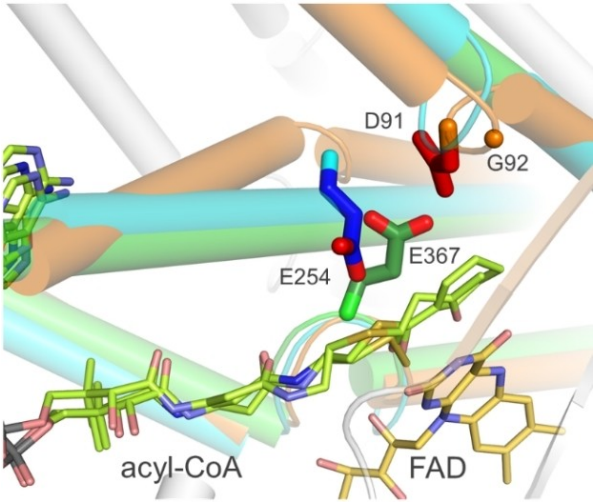

Figure 4. Active-site superposition of three ACAD-types characterized by the different origins of the catalytic acidic residue. Interrupted helices 79:98, 229:266, and 349:378 of Ch1DH are drawn in orange. The corresponding helices in human isovaleryl-CoA DH (1IVH) and butyryl-CoA DH of *Megasphera elsdenii* (1BUC) are shown in cyan and green, respectively. The carbons of the catalytic E254 and E367 are shown in blue and green. Due to high degree of overlay, only FAD of Ch1DH is shown. Conserved G92 of Ch1DH (Figure S2) is marked by a sphere. Bulkier side chains at residue 92 would implicate a clash between broken helix 79–98 and strand 120:123 (in wheat).

To substantiate the proposed function of individual active-site amino acids, a number of site-directed mutagenesis experiments were carried out (Table 1). The exchange of D91 by asparagine resulted in a substantial loss of the C3,C4- and C3,C6-dehydrogenation activities and thus strongly supports the role of the aspartate as catalytic base. In the D91E variant, a minor activity was retained with an inversed preference for the C3,C4- over C3,C6-dehydrogenation. To investigate the role of

Table 1. Dehydrogenation activities of molecular Ch1DH variants

Molecular variant	FAD/ monomer	Ch1DH activity[a] (C3,C6-DH)	Ch1,5DH activity[a] (C3,C4-DH)	ChDH activity[a] (C1,C2-DH)
Wild type	0.72	4,200 ± 200	890 ± 100	< 0.1
D91N	1.10	< 0.1	< 0.1	< 0.1
D91E	0.98	9 ± 3	34 ± 16	< 0.1
N241D	1.08	310 ± 30	270 ± 20	< 0.1
T363V	1.05	570 ± 30	670 ± 70	< 0.1
D91N + N241D	1.00	6 ± 2	11 ± 3	7 ± 3
D91N + T363C	0.68	< 0.1[b]	< 0.1[b]	0.4 ± 0.1[b]

[a] Activities given in nmol min^{-1} mg^{-1} (mean value ± standard deviation). [b] At pH 10.

the invariant N241 and T363 residues that replace the catalytic glutamate in C1,C2-dehydrogenating ACADs, we exchanged them by acidic amino acids. While the N241E variant was inactive, the N241D one showed a decreased activity, again with a shift towards C3,C4- vs C3,C6-dehydrogenation compared to the wild type; no C1,C2- dehydrogenation activity was found. The T363V mutant again preferred C3,C4- over C3,C6-dehydrogenation. Surprisingly, it showed highly decreased K_m-values for CH1CoA (2.5 μM vs. 31 μM) and Ch1,5CoA (5.7 μM vs. 85 μM). This, on the first view productive mutation was however accompanied by a profound decrease of the 3,6-dehydrogenation activity. Taken together, these results indicate that D91, N241, and T363 concertedly form a highly fine-tuned active site that is optimized to preferentially allow for the biologically relevant C3,C6- over the thermodynamically favored C3,C4-dehydrogenation.

To mimic the active site of a standard C1,C2-dehydrogenating ACAD, the D91 N/N241D double mutant Ch1DH was produced. Indeed, this variant gained a low but significant C1,C2-dehydrogenation activity; in parallel the C3,C6- and C3,C4-dehydrogenating activities were largely diminished. This finding indicates that the N91/D241 is competent to serve as catalytic base for proton abstraction at C3 and C1. The hydride transfer from C2 to N5 is geometrically feasible and no obstacle for the 1,2-dehydrogenation. The D91N/T363C variant completely lost the C3,C4- and C3,C6-dehydrogenating activities but retained a low but clearly detectable C1,C2-dehydrogenating activity at pH 10. At this pH, though far outside the optimal one near 7, the deprotonated cysteine thiolate can act as catalytic base.

The mutational studies indicate that Ch1DH is sensitive to subtle changes of the glutamate-replacing residues with regard to the overall activity and the preference for the C3,C6- over the C3,C4-dehydrogenation activity. This preference is essential for the biological role of Ch1CoA to form Ch1,5CoA as an intermediate of cyclohexane carboxylate degradation, whereas the aromatized benzoyl-CoA represents a dead-end product which is not part of the pathway (Figure S3). Thus, the challenging task of Ch1DH is both, to facilitate C3,C6-dehydrogenation and to suppress the aromatization-driven C3,C4-dehydrogenation. Though this is largely accomplished by the optimized isoalloxazine-N5-Ch1CoA-C6 and impaired N5-C4 geometries, the C3,C4-dehydrogenation could not be completely eliminated. In the cell, benzoyl-CoA formation will be further minimized by the conversion of the Ch1,5CoA intermediate by a highly active Ch1,5CoA hydratase and by further exergonic reactions of the degradation pathway (Figure S3).[23–25]

ACADs were previously considered to exclusively catalyze 1,2-dehydrogenation reactions of CoA esters in a conserved mechanistic manner. However, a non-canonical ACAD activity was recently described that forms a terminal alkene in a natural polyketide product by 3,4-dehydrogenation of an 1,2 dehydrogenated aliphatic acyl group.[11] Our work now provides molecular insights into a further expansion of the catalytic repertoire of ACADs. The 1,3-diene moiety formed by Ch1DH is generally recognized as a highly useful building block for the construction of diverse value-added chiral products by Diels-Alder cyclization and other reactions.[26] It provides an alternative biocatalytic route to the formation of conjugated cyclic dienes that are usually produced from feedstock arenes via Birch reduction, hydrogenation or other demanding dearomatization reactions.[27,28]

Acknowledgements

We thank Hartmut Michel for continuous support, the staff of the PXII-SLS beamline, Villigen, Switzerland for help during data collection as well as Barbara Rathmann and Yvonne Thielmann for operating the CrystalMation robot system. This work was funded by the Germany Research Foundation DFG within RTG 1976, project number 235777276 and the SPP1319 program (ER 222/5-1). Open Access funding enabled and organized by Projekt DEAL.

Conflict of Interest

The authors declare no conflict of interest.

Keywords: acyl-CoA dehydrogenases · enzyme catalysis · flavins · fatty acid oxidation · oxidoreductases

[1] Z. Swigoňová, A. W. Mohsen, J. Vockley, *J. Mol. Evol.* **2009**, *69*, 176–193.
[2] D. A. Pelletier, C. S. Harwood, *J. Bacteriol.* **2000**, *182*, 2753–2760.
[3] S. Wischgoll, M. Taubert, F. Peters, N. Jehmlich, M. Von Bergen, M. Boll, *J. Bacteriol.* **2009**, *191*, DOI 10.1128/JB.00205-09.
[4] R. Van Der Geize, K. Yam, T. Heuser, M. H. Wilbrink, H. Hara, M. C. Anderton, E. Sim, L. Dijkhuizen, J. E. Davies, W. W. Mohn, L. D. Eltis, *Proc. Natl. Acad. Sci. USA* **2007**, *104*, 1947–1952.
[5] M. Yang, R. Lu, K. E. Guja, M. F. Wipperman, J. R. St. Clair, A. C. Bonds, M. Garcia-Diaz, N. S. Sampson, *ACS Infect. Dis.* **2016**, *1*, 110–125.
[6] M. Warnke, C. Jacoby, T. Jung, M. Agne, M. Mergelsberg, R. Starke, N. Jehmlich, M. von Bergen, H.-H. Richnow, T. Brüls, M. Boll, *Environ. Microbiol.* **2017**, *19*, 4684–4699.
[7] P. C. Engel, V. Massey, *Biochem. J.* **1971**, *125*, 879.
[8] F. Li, J. Hinderberger, H. Seedorf, J. Zhang, W. Buckel, R. K. Thauer, *J. Bacteriol.* **2008**, *190*, 843–850.
[9] K. Watanabe, C. Khosla, R. M. Stroud, S. C. Tsai, *J. Mol. Biol.* **2003**, *334*, 435–444.
[10] J. D. Rudolf, L.-B. Dong, T. Huang, B. Shen, *Mol. BioSyst.* **2015**, *11*, 2717–2726.
[11] J. M. Blake-Hedges, J. H. Pereira, P. Cruz-Morales, M. G. Thompson, J. F. Barajas, J. Chen, R. N. Krishna, L. J. G. Chan, D. Nimlos, C. Alonso-Martinez, E. E. K. Baidoo, Y. Chen, J. W. Gin, L. Katz, C. J. Petzold, P. D. Adams, J. D. Keasling, *J. Am. Chem. Soc.* **2020**, *142*, 835–846.
[12] T. J. Erb, G. Fuchs, B. E. Alber, *Mol. Microbiol.* **2009**, *73*, 992–1008.
[13] S. Ghisla, C. Thorpe, *Eur. J. Biochem.* **2004**, *271*, 494–508.
[14] J. J. P. Kim, R. Miura, *Eur. J. Biochem.* **2004**, *271*, 483–493.
[15] C. Thorpe, J.-J. P. Kim, *FASEB J.* **1995**, *9*, 718–725.
[16] M. Schürmann, R. Meijers, T. R. Schneider, A. Steinbüchel, M. Cianci, *Acta Crystallogr. Sect. D* **2015**, *71*, 1360–1372.
[17] J. W. Kung, J. Seifert, M. von Bergen, M. Boll, *J. Bacteriol.* **2013**, *195*, 3193–3200.
[18] J. W. Kung, A.-K. Meier, M. Mergelsberg, M. Boll, *J. Bacteriol.* **2014**, *196*, 667–674.
[19] M. Boll, J. W. Kung, U. Ermler, B. M. Martins, W. Buckel, *J. Mol. Microbiol. Biotechnol.* **2016**, *26*, 165–179.
[20] K. P. Battaile, J. Molin-Case, R. Paschke, M. Wang, D. Bennett, J. Vockley, J. J. P. Kim, *J. Biol. Chem.* **2002**, *277*, 12200–12207.

[21] H. S. Toogood, A. van Thiel, J. Basran, M. J. Sutcliffe, N. S. Scrutton, D. Leys, *J. Biol. Chem.* **2004**, *279*, 32904–32912.
[22] R. D. Gandour, *Bioorg. Chem.* **1981**, *10*, 169–176.
[23] F. Peters, Y. Shinoda, M. J. McInerney, M. Boll, *J. Bacteriol.* **2007**, *189*, 1055–1060.
[24] J. W. Kung, A. K. Meier, M. Mergelsberg, M. Boll, *J. Bacteriol.* **2014**, *196*, 3667–3674.
[25] G. Fuchs, M. Boll, J. Heider, *Nat. Rev. Microbiol.* **2011**, *9*, 803–816.
[26] J.-A. Funel, S. Abele, *Angew. Chem. Int. Ed.* **2013**, *52*, 3822–3863; *Angew. Chem.* **2013**, *125*, 3912–3955.
[27] W. C. Wertjes, E. H. Southgate, D. Sarlah, *Chem. Soc. Rev.* **2018**, *47*, 7996–8017.
[28] S. P. Roche, J. A. Porco, *Angew. Chem. Int. Ed.* **2011**, *50*, 4068–4093; *Angew. Chem.* **2011**, *123*, 4154–4179.

Manuscript received: August 16, 2021
Revised manuscript received: September 15, 2021
Accepted manuscript online: September 23, 2021
Version of record online: September 30, 2021